 SDHM, vol.7, no.4, pp.283-296, 2011

Numerical Modeling and Simulation of a Bolted Hybrid Joint

F. Caputo, G. Lamanna and A. Soprano[1]

Abstract: The present paper deals with a numerical investigation on hybrid bolted joints between unidirectional, quasi isotropic Carbon Fiber Reinforced Polymer (CFRP) composite and aluminium alloy plates, subjected to traction loads. CFRP composite materials are widely used in aerospace applications, where requirements of weight reduction and structural high performances are very compelling. Composite materials generally present high resistance to fatigue and corrosion but the presence of joints in the structure can cause structural problems and then decrease the structural reliability of jointed component.

A hybrid bolted joint constituted of a metal plate, made of aluminium alloy, and a carbon fiber reinforced plastic (CFRP) composite plate has been analyzed; a titanium bolt holds the plates together. Experimental results have been compared with those obtained through a numerical analysis developed by using Abaqus® finite element code, in order to validate the numerical model.

Once the model has been validated, other suitable configurations have been numerically analyzed to investigate on the global strength of the examined hybrid joint for different geometrical configurations; in particular, the influence of bolt hole clearance on the stiffness and strength of the joint have been considered.

It has been found that the developed three-dimensional finite element model provides results, which are in good agreement with the experimental ones. Three-dimensional effects such as secondary bending and through-thickness variations in stress and strain are well represented by such model.

Keywords: Hybrid bolted joint, CFRP, bolt hole clearance.

1 Introduction

Carbon fiber reinforced polymer (CFRP) composites are widely used within the aerospace and automotive industries due to their very high specific strength and

[1] The Second University of Naples - DIAM, Naples, Italy.

stiffness properties. These materials have a high strength/weight ratio and can be used in many technical applications.

Generally, composite materials have a remarkable resistance to fatigue and corrosion, see Bickford J.H. (2008) and Tae Seong Lim, Byung Chul Kim, Dai Gil Lee (2006), but the jointing of components made of such materials can constitute a critical point in the design process of the overall structure, as well as it happens with metal components.

However, reaching the expected structural coupling efficiency by using composite materials is much more challenging than by using metals because of the low bearing and shear strengths, the high notch sensitivity, the dependence of the joint strength on laminate configuration and the influence of environment, so that those peculiarities constitute a limitation on the performance of composite structures, see Hoon, Young, Lee (97) and Jung, Choi (2006).

Different types of jointing techniques exist in the aerospace and automotive industries, among which bonding, riveting, brazing and bolting are the most widely diffused. In bolted joints, constituting the subject of the study developed in the present paper, a severe stress state characterizes the neighborhood of the jointing area (see Chen, Lee and Yeh 1995) and cracking phenomena can arise at the hole edge; this type of joint, however, shows a remarkable reliability and can be usefully adopted with several composites materials such as the already mentioned carbon fiber reinforced plastic (CFRP) or glass fiber reinforced epoxy (GFRE) composites, see Khashaba, Sallam, Al-Shorbagy and Seif (2006).

Carbon fiber reinforced polymer composites are subjected to various typologies of damage, which include matrix cracking, delamination and fiber breakage, see Kweon, Jung, Kim, Choi and Kim (2006). For composite laminates, delamination is one of the major concerns since it can reduce significantly the load carrying capacity of the laminate. Unlike metallic structures, which are homogenous and have the ability to dissipate energy through yielding, composite structures are relatively brittle and exhibit weak interlaminar strength.

As a consequence, even low velocity impacts on CFRP composites can introduce significant delamination defects, which are not visible from the external surfaces of the component.

There are many studies, based on analytical and numerical methods, which discuss how to predict and monitor the failure of a bolted joint, see Camanho and Lambert (2006) and Sancaktar (2001), and the propagation path of cracks around the bolted area, see Widagdo, Aliabadi (2001), or even the distribution of the load among the laminae; it has been found that one of the main causes of such cracking is the excessive closure force upon the bolts.

The present work deals with bolted joints; in particular the jointing of two components of different materials has been studied, the first one being a CFRP composite and the second one an aluminium alloy; the two elements are jointed by means of a titanium bolt.

The numerical simulation of the behaviour of a hybrid bolted joint subject to longitudinal traction load is described, which includes the study of the non linear behaviour of such materials; to achieve a good accuracy of the results from the numerical simulation, they have been compared with experimental results, in terms of strain values at different points of the jointed composite plates.

Furthermore, the relative displacement between the two plates, due to sliding effects, has also been analyzed and considered in the numerical-experimental comparison.

Once the model has been validated, other possible configurations have been numerically analyzed to investigate on the global strength of the examined hybrid joint for different geometrical configurations; in particular, the influence of bolt-hole clearance on the stiffness and strength of the joint have been considered, McCarthy C.T., McCarthy M.A. (2005), Yoon, Kim (2011).

2 Experimental testing

The joint which has been examined is made of two plates with different thicknesses and materials, whose mechanical properties are listed in Tab 1: the first one is made of 7475-T76 aluminium alloy, while the second one is made of CFRP composite, with a stacking sequence [($\pm$45,0,90)4]s.

Two different Ti6A114VSTA titanium bolt configurations (both with a 6 mm shank diameter) have been investigated, by considering a protruding head for the first one (head diameter: 9.9 mm; head height: 3.5 mm, see Fig. 1) and a countersunk type for the second one (maximum pin diameter: 12 mm; height of conical portion: 3 mm, see Fig. 2). The dimensions of the plates are 150 mm x 36 mm x 4/4.16 mm (metal/composite); both of them have a centered bolt hole, which is located at 18 mm from the end of the plate (Fig. 1). Reinforcement hasn't been provided on the aluminium plate around the countersunk hole, which is, of course, partially conical in order to house the head of the bolt (Fig. 2).

The clamping nut has a global height of 6.4 mm; it is partially conical and it fits with a washer with an external diameter of 10.8 mm and a height of 2 mm.

The laminates in the joint were made using Ciba-Geigy unidirectional prepreg system HTA/6376, while the bolt holes were machined using the special generation procedure developed at the Royal Institute of Technology in Stockholm, see Gaffney (1993).

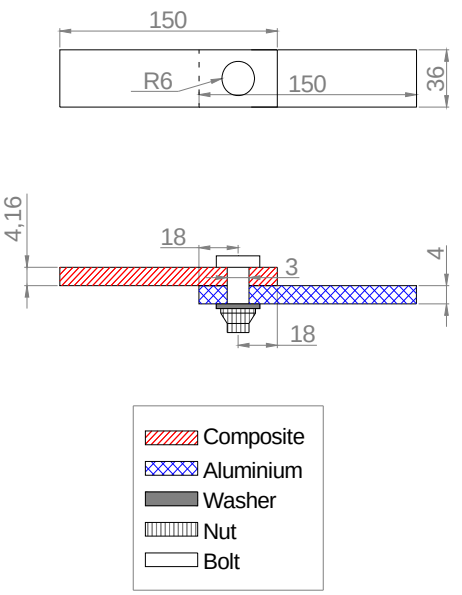

Figure 1: Specimen with protruding head bolt (measures in mm; drawing not scaled)

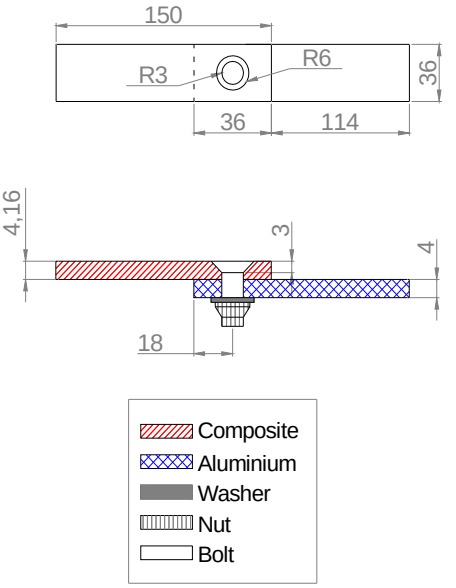

Figure 2: Specimen with countersunk hole (measures in mm; drawing not scaled).

In that procedure, the hole is generated with a grinding tool, rotating eccentrically about a principal axis and, at the same time, about its own axis. With this method, it is possible to create holes with high accuracy without causing delaminations and chip-outs.

All laminates were inspected by ultrasonic device to identify possible flaws due to the manufacturing process and, after hole machining, by X-ray; all specimens proved to be of good quality.

The adopted tolerance standard between bolt and hole was the ISO f7/H10 for both the examined configurations. The bolts were either tightened by a torque of 1mN (corresponding to finger-tightening), or fully tightened by a torque of 35 mN.

The specimens were equipped with strain gauges, as shown in Fig. 3, to compare the numerical results with the experimental ones.

Most of the gauges were located at the slip plane between the plates, where 0.8 mm deep slots were milled in the aluminum part to accommodate the gauges.

The gauges located at positions D and E on both sides of the laminate (Fig. 3) were of use to measure the secondary bending in the specimens caused by the

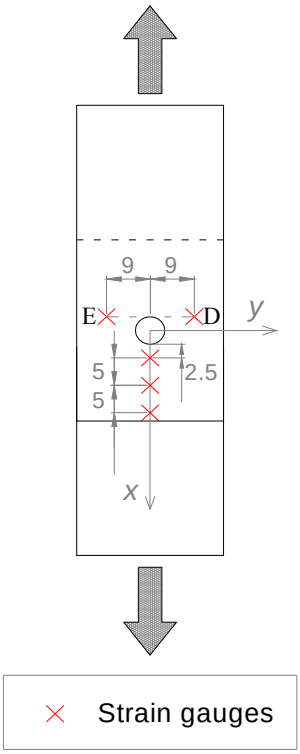

Figure 3: Strain gauges positioning (measures in mm).

Table 1: Mechanical properties

	E_{11} [GPa]	E_{22} [GPa]	E_{33} [GPa]
Ply properties	141	10	11
[(±45,0,90)4]S32	E_{12} [GPa]	E_{13} [GPa]	E_{23} [GPa]
Type:	5.2	5.2	3.9
quasi-isotropic	ν_{12}	ν_{13}	ν_{23}
	0.3	0.5	0.5

Aluminium	E [GPa]	ν
AA7475-T76	69	0.28
Titanium	E [GPa]	ν
Ti6A114VSTA	110	0.29

misalignment in the thickness direction of the loads applied at the end of the plates.

The deformation due to slipping across the fastener hole was measured with an extensometer, as shown in Fig. 4, which was attached to a pair of metal arms which were bonded to the laminate and to the aluminium plate at one side of the specimen.

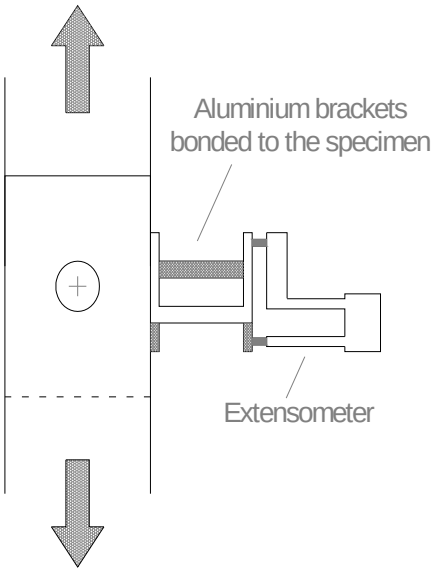

Figure 4: Extensometer installation.

In a few cases, the pre-tension in the fastener was measured using a special bolt with a cylindrical strain gauge installed on the axis of the shank (Fig. 5). Therefore, a 2 mm diameter hole was drilled through the bolt head along the axis of the shank; then, a 1.8 mm diameter cylindrical strain gauge was bonded into the hole in such a way that the centre of the gauge was placed in correspondence of the slip plane of the joint when the bolt was mounted.

To prevent secondary bending, some of the specimens were tested by also considering a special device, which laterally supported them as shown in Fig. 6. It was made of two rigid steel plates, which were bolted together by eight bolts, four on each side of the specimen; furthermore, each of the two plates had a circular hole to accommodate the bolt head and the nut of the tested joint and Teflon films were applied on the contact zone between the plates and the specimen, in order to reduce friction.

Following the procedures described by Ireman (1998), all tests were performed

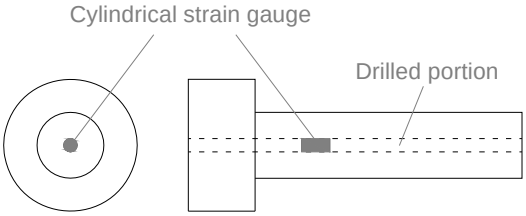

Figure 5: Bolt used for measurement of pre-tension.

at room temperature, with dry laminates (RT/AR conditions), by using an Instron 4505 hydraulic traction machine and applying the load at a constant loading speed of 1.0 mm/min.

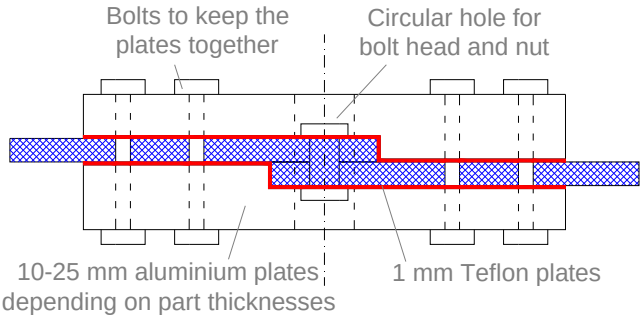

Figure 6: Experimental lateral support device.

3 Description of the numerical model

A finite element model representative of a single joint was built to simulate the tests and to provide numerical results to be compared with the experimental ones.

It was composed by the aluminium plate, the composite plate and by a special component, which grouped the washer, the nut and the bolt: therefore the contact stresses between nut and washer and between washer and aluminium plate could not be taken separately into account.

The model of the first component, i.e. the aluminium plate, consisted of 2,816 elements and 3,528 nodes and was entirely discretized by means of tridimensional first-order solid elements of the type C3D8, from Abaqus® library (Fig. 7), see Abaqus Analysis, user's manual.

That type of finite element is suitable for complex nonlinear analyses involving contact, plasticity and large deformations. Such elements can have just one integration point, which would reduce runtimes, but in that case it could happen that they would deform in such a way that the strains evaluated at the integration point are all zero, which, in turn, would lead to an uncontrolled distortion of the mesh (hourglassing). In order to avoid this effect, fully integrated elements were chosen.

The model of the composite plate had the same number of elements and nodes used to represent the aluminium plate and it was discretized by means of the same tridimensional first-order C3D8 solid elements, but, unlike the previous case, a composite solid section was associated to this component. In fact, that solid element can be constituted of a single homogeneous material, but it can also include several layers of different materials for the analysis of laminated composite.

In the Abaqus® code the use of composite solids is limited to three-dimensional brick elements that have only translational degrees of freedom; the thickness, the required number of section points for numerical integration through each layer and the material type and orientation associated to each layer are specified as a part of the composite solid section parameters.

There is one integration point for each layer and it is located in the middle of the layer thickness. All the layers have the same thickness.

The model of the third component, the bolt, consisted of about 6,848 elements and 7,874 nodes and had the same type of discretization of the aluminum plate but, of course, with different material properties (Table 1, Fig. 8).

The whole model consisted of about 12,500 elements and 15,000 nodes; the free end of the metal plate was clamped while a displacement was imposed to the free end of the composite plate to introduce a longitudinal traction load of 4 kN upon the specimen.

The modeling of the interface elements at the contact surfaces by means of the "node to surface" algorithm (with the "small sliding" option), completed the numerical model: six different interfaces were characterized in order to avoid undesired penetrations of the contact areas, see Whitney, Iarve and Brockman (2004). The friction coefficient was set to 0.15 at all contact surfaces.

In consideration of the type of bolt adopted, the tightening torque (T) of 1 m•N provided an axial load, $A = T \bullet f(\mu,\alpha,\beta,P,d_m) = 2.63$ kN, where μ = friction coefficient, α = helix slope, β = teeth angle, P = pitch, d_m = notch diameter.

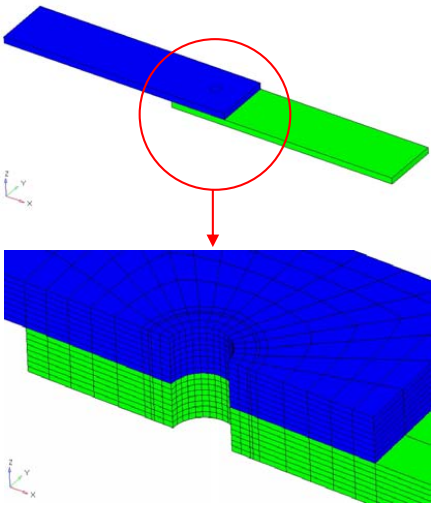

Figure 7: Discretization of aluminium and composite plates.

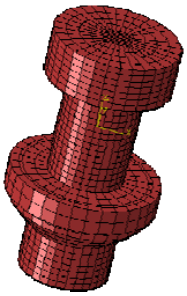

Figure 8: Protruding head bolt.

4 Results and discussion

Two different types of numerical results have been compared with the experimental ones: the relative displacement between the two plates (Fig. 9) and the total strains at different locations on composite plate, as it is shown in Fig. 10.

Fig. 11 shows a good agreement between numerical and experimental relative displacements; Fig. 12 and Tab. 2 confirm the good agreement of the numerical-experimental correlation in terms of total strains. The obtained results demonstrate that the virtual model provides accurate results, in spite of the difficulties encountered in the characterization of the composite material and in the calibration of the

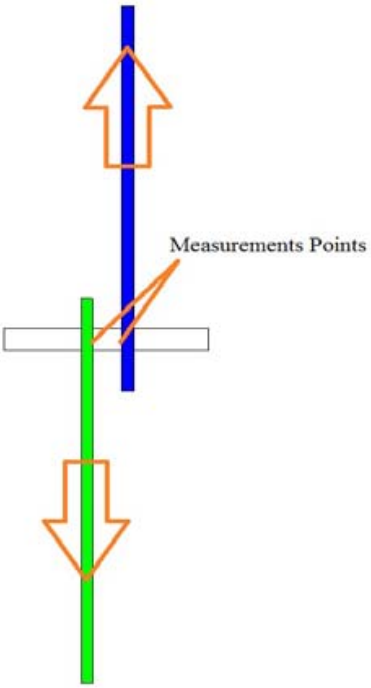

Figure 9: Relative displacement between two sheets

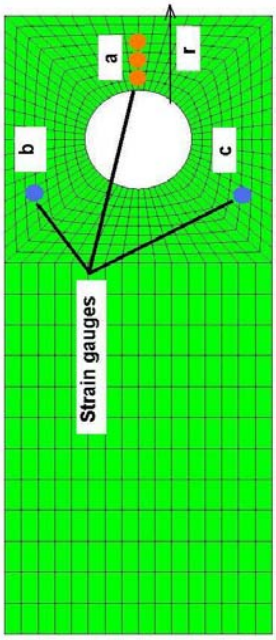

Figure 10: Gauges positioning

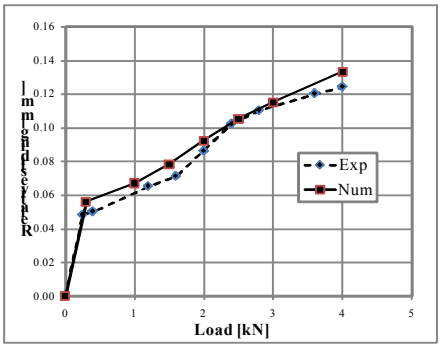

Figure 11: Relative displacement

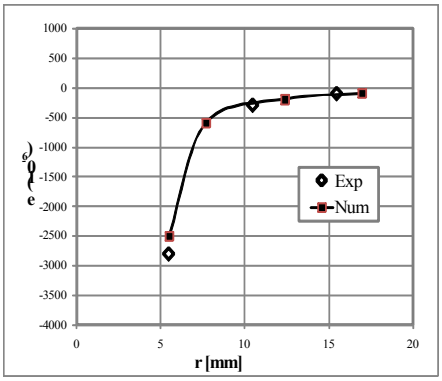

Figure 12: Strain at location “a”, load = 4 kN

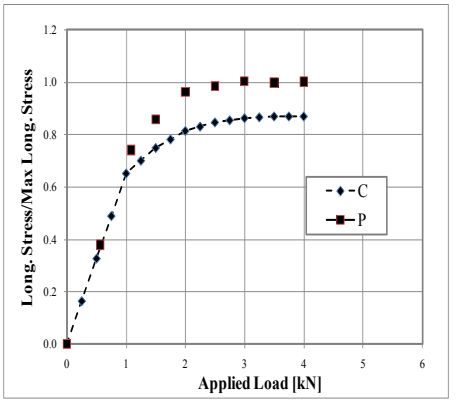

Figure 13: Relative stress for the different models P = protruding head bolt; C = countersunk head bolt

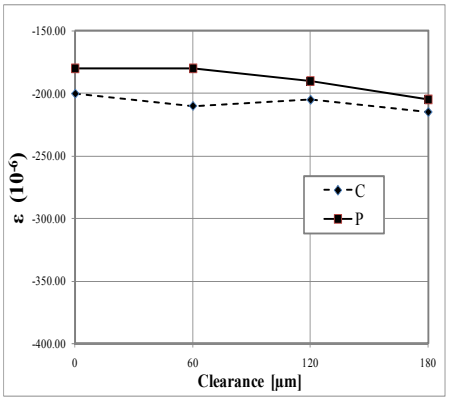

Figure 14: Strain at location "a" (x=12.4 mm, load = 4 kN). P = protruding head bolt; C = countersunk head bolt

several contact parameters involved in the model.

The lateral supports, introduced to prevent the secondary bending, did not show interesting results.

Trivial differences were observed in terms of relative sliding and total strains, when comparing the two models.

The validated model was modified in order to match the geometry of the countersunk bolt joint configuration and to analyze the influence of the bolt hole clearance on the strength of this type of joint.

Four different models with different clearance configurations have been also considered, ranging from neat-fit to 180 μm.

Comparing the stress results from the analyses of the two joint configurations, as illustrated in Fig. 13, it is possible to observe that the model with the protruding head is slightly stiffer than that one with the countersunk bolt (about 15%). This aspect comes from the more uniform contact fitting in the latter model.

The models have been built in accordance to Figg. 1 and 2, with quasi-isotropic and zero-dominated lay-ups.

Both protruding head and countersunk bolts have been analyzed; a 4 kN longitudinal traction load has been applied in all cases.

Within aerospace industry, 50-180 μm is a typical clearance range, therefore this paper considers clearances up to 3% of the hole diameter, with a fixed 6 mm shank

Table 2: Strains at locations "b" and "c", load = 4 kN

	Experimental	Numerical	Δ%
B location	1200	1230	+2.5%
C location	-500	-527	+5.2%

Table 3: Bolt-hole clearances

d_{nom}	Protruding – 6 mm	Countersunk – 6 mm
BOLT [μm] min - max	0	0
HOLE [μm] min - max	0	+60
	0	+120
	0	+180
bolt-hole CLEARANCE [μm]	0-180 (3% of 6mm diameter pin)	

diameter (Tab. 3).

The results show that the single-lap joint modeled with a protruding head bolt exhibits deformations which depend on the clearance value (Fig. 14), with a drop of 14% at a 180 μm gap (3% of hole diameter). The countersunk lap joint did not show a significant dependence on the clearance value.

5 Conclusions

The numerical model of the hybrid single lap joint considered within this work takes into account a lot of significant numerical aspects, such as contact algorithms, friction, axial closure force, stacking sequence, material calibration, bolt type, lateral support, clearance and element formulation. The general good agreement between numerical and experimental results established that the numerical model is rather robust and that it can be used for further investigations on this type of mechanical joints.

The good numerical model allowed the authors to provide a series of comparisons with the experimental results. The same numerical model could represent a valid numerical tool, both to forecast the damage initiation in hybrid bolted joints and to evaluate the stress-strain state of more complex assemblies. Furthermore, it could be integrated according to a more general numerical procedure of stochastic design improvement (SDI) to optimize some design characteristics, such as to reduce, for instance, the costs of production related to the hybrid bolted joints.

The countersunk joint introduces a distribution of the stresses along the contact surfaces which is much more uniform than in the joint with a protruding head bolt. This effect makes it less sensitive to the variation of the axial clearance value be-

tween pin and hole, as shown in the previous graphs, but a joint provided with such flared holes needs a more expensive manufacturing process.

One of the main causes of damage of composite bolted joints is related to an excessive value of the tightening torque of the bolts. It determines a very high axial closure force between the bolt and the plate and helps to arrest the cracks in the zone around the bolts. Because of such effects it can be opportune to perform numerous traction tests of the joint by varying the tightening torque of the bolts. This aspect of the research activity represents a very important feature for the authors.

Even if the strains, as computed in this work, did not show to be appreciably dependent on the clearance, Fig. 14 shows a notable difference between the models with protruding and countersunk head bolt. That effect can be connected to the lower strength of the countersunk head bolt, which, in presence of larger clearances, provides irregularities in the bolt hole contact, resulting in higher strain values. This effect may not result in practical consequences for the design of joints under in-service loads, but could be of interest in the case of joints designed to absorb energy (e.g. in crashworthy structures).

It has been found that the developed three-dimensional finite element models of the considered hybrid bolted joints, running in an acceptable computation time on a standard PC (ca 30 min. on intel 9400Q, ram 4GB), provided results which are in good agreement with the experimental ones. Three-dimensional effects such as secondary bending and through-thickness variations in stress and strain are well represented by such models.

References

Abaqus Analysis (2010): User's Manual: Abaqus, Inc. Dassault Systèmes, *USA*.

Bickford J.H. (2008): Introduction to the design and behavior of bolted joints. *CRC Press Taylor and Francis Group, Boca Raton FL, USA*.

Camanho P.P.; Lambert M. (2006): A design methodology for mechanically fastened joints in laminated composite materials. *Compos Sci Technol*, vol. 66, pp. 3004-3020.

Dal-Woo Yung; Nak-Sam Choi (2006): Characteristic fracture assessment of a rivet joint for hybrid composite laminates under static and fatigue shear loads. *Key Eng Mat,* vol. 326-328, pp. 1757-1760.

Erol Sancaktar; American Society of Mechanical Engineers. Design Engineering Division (2001): Threaded and riveted connections, design issues, reliability, stress analysis, and failure prevention. *Proceedings of ASME-IMECE conf.*, Edit. By ASME, New York.

Gaffney R. (1993): Three-dimensional finite element analysis of bolted composite lap joints. *Report 93-13, Royal Institute of Technology, Stockholm.*

Ireman T. (1998): Three-dimensional stress analysis of bolted single-lap composite joints. *Compos Struct*, vol. 41, pp. 195-216.

Ji Hoon Oh; Young Goo Kim; Dai Gil Lee (1997): Optimum bolted joints for hybrid composite materials. *Compos Struct,* vol. 38, pp. 329-341.

Khashaba U.A.; Sallam H.E.M.; Al-Shorbagy A.E.; Seif M.A. (2006): Effect of washer size and tightening torque on the performance of bolted joints in composite structures. *Compos Struct*, vol. 73, pp 310-317.

Kweon J.H.; Jung J.W.; Kim T.H.; Choi J.H.; Kim D.H. (2006): Failure of carbon composite-to-aluminium joints with combined mechanical fastening and adhesive bonding. *Compos Struct*, vol. 75, pp. 192-198.

McCarthy C.T.; McCarthy M.A. (2005): Three-dimensional ?nite element analysis of single-bolt, single-lap composite bolted joints: Part II—-effects of bolt hole clearance. *Compos Struct,* vol. 72, pp. 159-175.

Tae Seong Lim; Byung Chul Kim; Dai Gil Lee (2006): Fatigue characteristics of the bolted joints for unidirectional composite laminates. *Compos Struct,* vol. 72, pp. 58-68.

Tae Ho Yoon; Seung Jo Kim (2011): Refined numerical simulation of three-dimensional riveting in laminated composites. *J Aircraft,* vol. 48, no. 4, pp. 1434-1443.

Wen-Hwa Chen; Shyh-Shiaw Lee; Jyi-Tyan Yeh (1995): Three-dimensional contact stress analysis of a composite laminate with bolted joint. *Compos Struct,* vol. 30, pp. 287-297.

Widagdo D. ; Aliabadi M.H. (2001): Boundary element analysis of cracked panels repaired by mechanically fastened composite patches. *Eng Anal Bound Elem,* vol. 25, pp. 339-345.

Whitney T.J.; Iarve E.V.; Brockman R.A. (2004): Singular stress fields near contact boundaries in a composite bolted joint. *Int J Solid Struct*, vol. 41, pp. 1893-1909.